Science of the Total Environment 705 (2020) 135912

Contents lists available at ScienceDirect

Science of the Total Environment

journal homepage: www.elsevier.com/locate/scitotenv

Integrative assessment of low-dose gamma radiation effects on *Daphnia magna* reproduction: Toxicity pathway assembly and AOP development

You Song [a,b,*], Li Xie [a,b,c], YeonKyeong Lee [b,d], Dag Anders Brede [b,c], Fern Lyne [b,e], Yetneberk Kassaye [b,c], Jens Thaulow [a,b], Gary Caldwell [e], Brit Salbu [b,c], Knut Erik Tollefsen [a,b,c]

[a] Norwegian Institute for Water Research (NIVA), Gaustadalléen 21, N-0349 OSLO, Norway
[b] Centre for Environmental Radioactivity (CERAD), Norwegian University of Life Sciences (NMBU), Post box 5003, N-1432 Ås, Norway
[c] Norwegian University of Life Sciences (NMBU), Faculty of Environmental Sciences and Natural Resource Management (MINA), P.O. Box 5003, N-1432 Ås, Norway
[d] Norwegian University of Life Sciences (NMBU), Faculty of Biosciences, P.O. Box 5003, N-1432 Ås, Norway
[e] Newcastle University, Newcastle upon Tyne, UK

HIGHLIGHTS

- Low-dose ionizing radiation-mediated reproductive effects are poorly understood
- Initial effort to systematically assess the effects of gamma radiation on *Daphnia*
- Integrated biotesting approaches to measure effects at multiple biological levels
- Non-monotonic dose-responses and multiple toxicity pathways identified in *Daphnia*
- First Adverse Outcome Pathways proposed for radiation and aquatic organisms

GRAPHICAL ABSTRACT

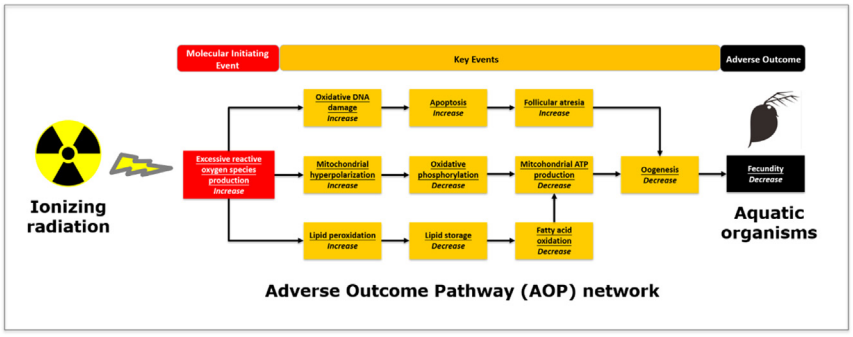

ARTICLE INFO

Article history:
Received 12 August 2019
Received in revised form 25 November 2019
Accepted 1 December 2019
Available online 5 December 2019

Editor: Dr. Henner Hollert

Keywords:
Ionizing radiation
Crustacean
Reproduction
Oxidative stress
Mechanism of action
Adverse outcome pathway

ABSTRACT

High energy gamma radiation is potentially hazardous to organisms, including aquatic invertebrates. Although extensively studied in a number of invertebrate species, knowledge on effects induced by gamma radiation is to a large extent limited to the induction of oxidative stress and DNA damage at the molecular/cellular level, or survival, growth and reproduction at the organismal level. As the knowledge of causal relationships between effects occurring at different levels of biological organization is scarce, the ability to provide mechanistic explanation for observed adverse effects is limited, and thus development of Adverse Outcome Pathways (AOPs) and larger scale implementation into next generation hazard and risk predictions is restricted. The present study was therefore conducted to assess the effects of high-energy gamma radiation from cobalt-60 across multiple levels of biological organization (i.e., molecular, cellular, tissue, organ and individual) and characterize the major toxicity pathways leading to impaired reproduction in the model freshwater crustacean *Daphnia magna* (water flea). Following gamma exposure, a number of bioassays were integrated to measure relevant toxicological endpoints such as gene expression, reactive oxygen species (ROS), lipid peroxidation (LPO), neutral lipid storage, adenosine triphosphate (ATP) content, apoptosis, ovary histology and reproduction. A non-monotonic pattern was consistently observed across the levels of biological organization, albeit with some variation at the lower end of the dose-rate scale, indicating a complex response to radiation doses. By integrating results from different bioassays, a novel pathway network describing the key toxicity pathways involved in the reproductive

* Corresponding author at: Norwegian Institute for Water Research (NIVA), Gaustadalléen 21, N-0349 Oslo, Norway.
E-mail address: you.song@niva.no (Y. Song).

https://doi.org/10.1016/j.scitotenv.2019.135912

effects of gamma radiation were proposed, such as DNA damage-oocyte apoptosis pathway, LPO-ATP depletion pathway, calcium influx-endocrine disruption pathway and DNA hypermethylation pathway. Three novel AOPs were proposed for oxidative stressor-mediated excessive ROS formation leading to reproductive effect, and thus introducing the world's first AOPs for non-chemical stressors in aquatic invertebrates.

1. Introduction

Regulatory and public concerns for the environmental impact of ionizing radiation have been raised after major nuclear events such as the Chernobyl and Fukushima accidents. Following the Chernobyl accident, 3–4 tons of spent nuclear fuel containing a series of radionuclides (fission products, activation products, transuranics such as Pu-isotopes) were released, including the long-lived radionuclides including ^{137}Cs and ^{90}Sr (Valković, 2019). Following the Fukushima accident, the release was dominated by the long-lived ^{137}Cs and the short-lived ^{131}I gamma emitters (Steinhauser et al., 2014). As also observed at other sites contaminated from nuclear accidents or from nuclear weapons tests, long-lived radionuclides such as ^{137}Cs (gamma emitter), ^{90}Sr (beta emitter), and Pu-isotopes (e.g., ^{240}Pu, ^{239}Pu, alpha emitters) are the key radiation dose contributors, thus posing potential long-term hazards to humans and wildlife in contaminated areas (Cochran et al., 1993; Kryshev et al., 1997; Beresford and Copplestone, 2011; Steinhauser et al., 2014).

Crustaceans are key primary consumers (herbivores) connecting primary producers and higher consumers (carnivores) in many food webs (Burns and Schallenberg, 1996; Covich et al., 1999). Aquatic crustaceans such as the water flea *Daphnia magna* have been widely used as indicators for ecosystem health and as standard species in regulatory toxicity tests for ecological hazard and risk assessment (OECD, 2012). Freshwater crustaceans such as *Asellus aquaticus* and *Daphnia* occur in contaminated lakes and ponds in Chernobyl (Fuller et al., 2017; Goodman et al., 2019), with the frequency of studies on the adverse effects of ionizing radiation increasing over the past decades to reflect their high ecological relevance (reviewed in Dallas et al. (2012) and Fuller et al. (2015)).

The hazards of chronic exposure to low-dose ionizing radiation have been well documented for several crustacean species in both laboratory and field studies (reviewed in Fuller et al. (2015)). Adverse effects such as reduced reproduction, reduced body mass, altered molting patterns, reduced reproduction and reduced offspring fitness are tightly associated with chronic ionizing radiation exposure (reviewed in Dallas et al. (2012) and Fuller et al. (2015)). The modes of action (MoAs) of ionizing radiation in crustaceans are considered to be similar to those reported for vertebrates (Song et al., 2014) and plants (Xie et al., 2019), with DNA damage due to ionization and excitation of water molecules, induction of free radicals, recombination and production of reactive oxygen species (ROS), or less probably due to direct hit on DNA molecules, representing two initial events. Various downstream events, such as altered transcriptional regulation involved in antioxidant defense and DNA repair, lipid peroxidation, mitochondrial dysfunction, programmed cell death and transgenerational epigenetic effects have also been documented (Gomes et al., 2018; Trijau et al., 2018). Despite a series of dose-response experiments having been performed and a number of endpoints (e.g. DNA damage and lipid peroxidation) extensively studied, there is a lack of mechanistic understanding as to how these effects are causally linked in toxicity pathways, leading to adverse effects relevant for ecological health and safety assessments.

Portraying causal linkages between the molecular initiating event (MIE) of a stressor, key events (KE) at increasing levels of biological organization and adverse outcome (AO) at the individual or population level as the Adverse Outcome Pathway (AOP) framework is becoming increasingly useful in regulatory toxicology (Ankley et al., 2010; Tollefsen et al., 2014). However, the current AOP framework is highly chemical- and vertebrate-centric. Development of AOPs for non-chemical stressors such as ionizing radiation, and for ecologically relevant species such as aquatic crustaceans is particularly important for the full implementation of the AOP framework for next generation ecological hazard and risk assessment of various environmental stressors (Fay et al., 2017; Song et al., 2017).

The present study was therefore conducted to develop novel AOPs for understanding ionizing radiation-mediated reproductive effects in aquatic organisms, using external gamma radiation as the model stressor, and the water flea *Daphnia magna* as the prototypical species. Reproduction was chosen as the apical (adverse) endpoint due to its importance for population health in the ecosystems and high relevance for ecological risk assessment. By integrating multiple bioassays, this study aimed to: 1) generate new mechanistic knowledge on gamma radiation-mediated effects at different levels of biological organization; 2) propose a novel toxicity pathway network for ionizing radiation-mediated reproductive effects; and 3) develop the world's first AOPs for conceptualizing oxidative stressor-mediated reproductive effects in aquatic organisms.

2. Materials and methods

1.1 *Daphnia* culture

Daphnia magna (DHI strain, DHI Water Environment Health, Hørsholm, Denmark) were cultured in M7 medium (pH 7.8 ± 0.2, 50 mL medium/daphnid) in a climate room (20 ± 1 °C and 16 h light: 8 h dark) at Norwegian Institute for Water Research (NIVA). The culture medium was renewed twice per week. Immediately following medium renewal, juveniles were removed and the concentrated unicellular green algae *Raphidocelis subcapitata* (corresponding to 200 μg carbon per daphnid per day) was added as food for the daphnids (OECD, 2012).

1.2 Gamma exposure and sampling

The external colbalt-60 (8 Ci) gamma radiation exposure was conducted at the FIGARO irradiation facility NMBU, Ås, Norway (Lind et al., 2019). Nominal does-rates were calculated based on calibrated field dosimetry (Bjerke and Hetland, 2014). Samples were positioned at distances according to measured dose-rates to water (Dw) using nanoDot™ (Landauer, Glenwood, USA), as previously described (Gomes et al., 2018). Seven gamma dose-rates, control (background), 0.4, 1, 4, 10, 40 and 100 mGy/h were applied. pH of the medium was measured before and after the exposure using a WTW multi-parameter portable meter MultiLine® Multi 3420 coupled with a WTW SenTix® pH electrode with temperature sensor (Xylem Analytics, Weilheim, Germany). The same multi-parameter meter was also used to measure dissolved oxygen (DO) coupled with a WTW-optical IDS dissolved oxygen sensor FDO® 925 (Xylem Analytics). Two *Daphnia* exposure protocols were used to capture both adverse outcomes of relevance and mechanistic endpoints. The first protocol involved a modified OECD TG211 *Daphnia magna* Reproduction Test (OECD, 2012) for determination of the apical effects (i.e. mortality, molting frequency, ovulation frequency and reproductive output). Briefly, individual neonates (<24 h old, $n = 5$–10 due to limited gamma beam width) were placed in a plastic beaker containing 45 mL M7 medium and exposed to gamma radiation for 21 days. The test organisms were fed daily with *R. subcapitata* and the test media were renewed every two days. Observations on

individual responses were made daily, including the number of survivors, number of old cuticles at the bottom of the beaker, presence or absence of new eggs in the brood chamber and number of neonates. The neonates were removed prior to feeding to avoid crowding effects. Individual daphnids were sampled after 14- and 21-day exposures fixed in 1 mL Bouin's fluid (Sigma-Aldrich, St. Louis, USA) and stored at 4 °C for histopathological analysis; The second protocol involved a short-term (8-day) test to understand early toxicological events in *D. magna* leading to reproductive effects at a later stage. Briefly, ten neonates (<24 h old) were placed in a plastic beaker containing 45 mL M7 medium ($n = 5$–10 due to limited beam width) and exposed to gamma radiation for 8 days. The 8-day exposure protocol was chosen as the juvenile developmental stage was considered susceptible to ionizing radiation. After 8 days, the majority of the daphnids were in the transition period from adolescents to adults where the first batches of embryo were visible (but not released). The early toxicological events measured could therefore be linked to changes in reproductive strategies. The 8-day test was repeated four times to ensure sufficient material for subsequent downstream analyses: a) three daphnids were pooled and stored in RNALater (Qiagen, Hilden, Germany) for transcriptional analysis ($n = 5$); b) individual daphnids were sampled and immediately used (1 daphnid per replicate) for measurements of different types of ROS ($n = 4$), mitochondrial inner membrane potential (MMP, $n = 3$), lipid storage (n = 3) and apoptosis ($n = 6$); c) pooled daphnids (6 individuals per replicate) were stored in liquid nitrogen for measurement of lipid peroxidation (n = 5); d) two daphnids were pooled and stored in liquid nitrogen for measurement of whole-body ATP content (n = 3). The length of individual daphnid used in different functional bioassays were measured and converted to estimated weight using a published length-weight regression model (Cauchie et al., 2000) for data normalization.

1.3 Transcriptional analysis

Total RNA was extracted using the RNeasy Plus Mini kit (Qiagen) following the manufacturer's instructions. The purity and yield of the RNA samples were immediately assessed using a spectrophotometer (Nanodrop® ND-1000, Nanodrop Technologies, Wilminton, Delaware, USA). The RNA integrity was checked using an Agilent Bioanalyzer and RNA 6000 Nano chips (Agilent Technologies, Santa Clara, California, USA) according to the manufacturer's protocol. Intact RNA samples (clear peaks of RNA and flat bottom) with high purity (260/280 > 1.8) and sufficient yield (>500 ng) were stored at −80 °C until use.

Quantitative real-time reverse transcription polymerase chain reaction (qPCR) was used to determine the transcriptional changes in a selection of *D. magna* biomarker genes representing different toxicological functions. Primer sequences (Appendix, Table A1) were designed using the online software Primer3 v4.0.0 (http://primer3.ut.ee/) and purchased from Invitrogen™ (Carlsbad, California, USA). The qPCR assay ($n = 5$) was performed using a Bio-Rad CFX384 platform (Bio-Rad Laboratories, Hercules, CA), as previously described (Song et al., 2016). A standard curve was generated using a dilutions series of pooled cDNA (1.25, 2.5, 5, 10, 20 ng) from all samples in this analysis for calculation of amplification efficiency and correlation coefficient. A qPCR amplification with an efficiency in the range of 90–105% and $R^2 > 0.98$ was considered valid for downstream data analysis. The relative expression of the target gene was calculated based on the threshold cycle (Cq) value using the Pfaffl Method (Pfaffl, 2001), and normalized to the geometric mean expression of glyceraldehyde 3-phosphate dehydrogenase (*Gadph*), beta actin (*β-actin*) and cyclophilin (*Cyp*) using the ΔΔCq method (Vandesompele et al., 2002).

1.4 ROS assays

Three fluorescent ROS probes, 2′,7′-dichlorodihydrofluorescein diacetate (H_2DCFDA), dihydrorhodamine 123 (DHR123) and BODIPY (Thermo Fisher Scientific), were used to detect whole-organism cellular, mitochondrial, and lipid peroxidation-related ROS in *D. magna*, respectively. Stock solutions of the probes (5 mM) were prepared in dimethyl sulfide (DMSO, *in vitro* grade, Sigma-Aldrich) and stored at −20 °C in the dark until use. Prior to analysis, the ROS probes were diluted in the culture (M7) medium as working solutions. The ROS assays ($n = 4$ for H_2DCFDA and DHR123, $n = 3$ for BODIPY) were performed as previously described (Gomes et al., 2018). Briefly, individual daphnids were placed in 200 μL M7 medium containing 5 μM probe in separate wells of a 96-well black microplate (Corning Costar, Cambridge, MA, USA). The plate was incubated for 1 h at room temperature in the dark. After incubation, the daphnids were washed three times with clean culture medium to remove excessive probes in the wells. The plates were immediately scanned using a VICTOR 3 microplate reader (PerkinElmer, Waltham, USA) with excitation/emission wavelengths of 485/538 nm. The results were normalized to the weight of individual *D. magna* calculated from the measured length according to the length-weight regression model proposed for this species (Cauchie et al., 2000).

1.5 Lipid peroxidation assay

Lipid peroxidation (LPO) was measured using the Lipid Peroxidation (malondialdehyde/MDA) Assay Kit (Abcam, Cambridge, UK) according to the principles of the thiobarbituric acid reactive substances (TBARS) method (Janero, 1990; Barata et al., 2005). Briefly, pooled daphnids ($n = 5$) were homogenized in 303 μL lysis solution (300 μL MDA lysis buffer +3 μL butylated hydroxytoluene/BHT) using a Precellys orbital shaker bead mill (Bertin Technologies, Montigny-le-Bretonneux, France). The homogenate was centrifuged at 13,000*g* for 10 min and 200 μL of clear supernatant was transferred to a new centrifuge tube. The MDA standards (0.32, 1.6, 8, 40, 200, 1000, 5000 nmol) were made by diluting the concentrated (4.17 M) MDA in double-distilled water (ddH2O) and used to generate a standard curve. To generate the MDA-TBA adduct, each sample or standard was mixed with 600 μL TBA reagent and incubated at 95 °C for 60 min. After incubation, the samples were cooled on ice for 10 min and transferred to a 96-well black microplate (Corning Costar). The absorbance (OD 532 nm) was measured using a VersaMax™ absorbance microplate reader (Molecular Devices, San Jose, USA). The amount of MDA in each sample was calculated based on the standard curve and further normalized to the calculated weight of *D. magna*.

1.6 Lipid storage assay

The Nile red fluorescent probe (Sigma-Aldrich) was used to detect lipid droplets (triacylglycerols) as an indicator of neutral lipids storage in *D. magna*. The assay was conducted according to (Jordao et al., 2015), with modifications. Briefly, a stock solution of 1.5 mM Nile red was prepared in DMSO and stored at −20 °C in the dark. Shortly before use, the stock solution was diluted in M7 medium to make a final working concentration of 1.5 μM. Individual daphnids ($n = 3$) were incubated in 200 μL of Nile red working solution in separate wells of a 96-well black microplate (Corning Costar) at room temperature in the dark for 1 h. The assay was run in technical duplicates to allow both quantification and imaging of lipid droplets. After incubation, the animals were washed three times with clean M7 medium to eliminate excess Nile red in the assay solutions. One set of technical replicates were transferred to 1.5 mL centrifuge tubes prior to removing the residual medium and adding 300 μL of isopropanol (Sigm-Aldrich). The animals were then homogenized using a Precellys orbital shaker bead mill (Bertin). After homogenization, the tubes were centrifuged at 10,000*g* for 5 min. The resulting supernatant (200 μL) was transferred to a new 96-well black microplate and measured using a VICTOR 3 microplate reader (PerkinElmer) with excitation/emission wavelength of 530/590 nm. The results were normalized to the calculated weight of *D. magna*.

1.7 Mitochondrial membrane potential assay

The mitochondrial MMP as an indicator of oxidative phosphorylation (OXPHOS) was measured using the fluorescent probe tetramethylrhodamine methyl ester perchlorate (TMRM, Thermo Fisher Scientific). Stock solutions (5 mM) were prepared in DMSO and stored at −20 °C in the dark until further use. Shortly before analysis, the stock solution was diluted in M7 medium to make a final working concentration of 2 μM. Individual daphnids ($n = 5$) were incubated in 200 μL TMRM working solution in separate wells of a 96-well black microplate (Corning Costar) at room temperature in the dark for 1 h. After incubation, the animals were washed three times with M7 medium to eliminate excess TMRM in the assay solutions. The plate was immediately scanned using a VICTOR 3 microplate reader (PerkinElmer) with excitation/emission wavelength of 530/590 nm. The results were normalized to the calculated weight of *D. magna*.

1.8 ATP assay

The total ATP content was quantified using the Luminescent ATP Detection Assay Kit (Abcam) following the manufacturer's protocol. Briefly, pooled (2 individuals) *D. magna* ($n = 3$) were homogenized in 225 μL lysis buffer (75 μL detergent +150 μL ddH_2O) using a Precellys orbital shaker bead mill (Bertin). The homogenate was centrifuged at 13,000*g* (4 °C) for 5 min. The supernatant (200 μL) was carefully transferred to a new tube. The ATP standards (0.00064, 0.0032, 0.016, 0.08, 0.4, 2, 10 μM) were prepared by diluting an ATP stock solution (10 mM) in the ATP assay buffer to generate a standard curve. Each sample or standard (150 μL) was mixed with 50 μL substrate solution in a 96-well black microplate (Corning Costar). The plate was shaken (600–700 rpm) for 5 min using an orbital shaker and incubated in the dark for another 10 min. The luminescence was immediately measured using a MicroBeta2 microplate counter (PerkinElmer). The total ATP content (nmol) in each sample was calculated based on the standard curve and further normalized to the calculated weight of *D. magna*.

1.9 Apoptosis assay

Terminal deoxynucleotidyl transferase dUTP nick end labeling (TUNEL) assay in combination with nucleus staining with propidium iodide (PI, Sigma-Aldrich) was used to identify apoptotic cell death in *D. magna*. Preparation of *D. magna* followed a modified method by (Ianora et al., 2004). *Daphnia magna* ($n = 6$) were fixed in 0.2 M NaCl and 4% paraformaldehyde in phosphate-buffered saline (PBS) overnight at 4 °C. To allow permeability, *Daphnia magna* was rinsed in PBS before being dipped in liquid nitrogen to fracture the carapace. The samples were then incubated in 20 μg/mL of proteinase K solution (Sigma-Aldrich) at 37 °C for 24 h. The TUNEL assay was performed using the In Situ Cell Death Detection Kit, (Sigma-Aldrich), according to the manufacturer's instructions. *Daphnia magna* was then incubated for 30 min at room temperature in 0.5 μg/mL propidium iodide (Ianora et al., 2004). Fluorescent images were taken using the Leica DM6B (Leica Microsystems, Wetzlar, Germany) fluorescent microscope, and the fluorescent intensity quantified using ImageJ v1.52a (https://imagej.nih.gov/ij/index.html).

1.10 Histopathological analysis

At the end of the exposure, the daphnids were immediately fixed in Bouin's fluid (Sigma-Aldrich, St. Louis, USA). Afterwards, the samples were kept at 4 °C overnight. The samples were washed with phosphate buffered saline (PBS, pH 7) after fixation and calcified in 5% hydrogen chloride (HCl) for 30 min. The calcified samples were washed with distilled water and post fixed in osmium tetraoxide (OsO4) for 30 min. Then, the samples were washed with PBS and water briefly and dehydrated in graded ethanol series. The samples were infiltrated in 1:1 LR White:ethanol (*v*/v, London Resin Company, England) overnight and followed by 4 h in 2:1 LR White:ethanol (*v*/v) and pure LR White for 2 days. The samples were then embedded in the pure LR white and polymerized at 60 °C overnight. Embedded samples were sectioned into 1 μm thickness using an Ultracut microtome (Leica EM UC6, Germany) and stained with toluidine blue O (Sigma-Aldrich). The stained samples were examined using a light microscope DM6B (Leica, Germany).

2.1. Statistical analysis

Statistical analyses were performed in Graphpad Prism v7 (Graphpad Software Inc., San Diego, USA). Outliers were identified and removed using the ROUT test (Motulsky and Brown, 2006) in Graphpad. Normal distribution and equal variance were checked prior to one-way analysis of variance (ANOVA) in combination with the Tukey post-hoc test. Data that failed to meet the prerequisites for ANOVA were analyzed using the Kruskal-Wallis non-parametric test followed with Dunn's post-hoc test. Pearson pair-wise correlation matrix was computed for all endpoints using the built-in function in Graphpad. In addition, a principle component analysis (PCA) was conducted using the R (v3.6.0, https://www.r-project.org/) statistical package factoextra (https://rpkgs.datanovia.com/factoextra/index.html) to identify coherence between different types of response. A probability (p) level of 0.05 was applied to all statistical tests.

3. Results

1.11 Exposure quality control

The medium had pH of 8.0 ± 0.2 and dissolved oxygen higher than 9 mg/L throughout the exposure. Gamma radiation dosimetry showed good correspondence between nominal and measured gamma dose-rates (Appendix, Table A2), with average measured dose-rates of 0.4, 0.9, 3.8, 11.6, 42.9 and 95.7 mGy/h. The lead-shielded controls had an average scattered (background) radiation dose-rate of 0.005 mGy/h.

1.12 Transcriptional responses

The majority of the biomarker genes displayed non-monotonic responses to gamma radiation (Fig. 1). Genes such as catalase (*Cat*), glutathione S-transferase (*Gst*), DNA repair protein RAD50 (*Rad50*), DNA directed polymerase REV1 (*Rev1*), apoptosis-inducing factor 3 (*Aifm3*), TP53-regulated inhibitor of apoptosis 1 (*Triap*), 5-amp-activated protein kinase catalytic subunit alpha (*Ampk*), NADH dehydrogenase (ubiquinone) 20 kDa subunit (*Nd20l*), calmodulin (*Calm*), ecdysone receptor B (*EcRb*), methoprene tolerant (*Met*), DNA (cytosine-5)-methyltransferase 1 (*Dnmt1*), DNA (cytosine-5)-methyltransferase 3A2 (*Dnmt3a2*) displayed consistent non-monotonic up-regulation, with an increase in expression from 0 (control) to 4 mGy/h (phase 1), followed by a clear reduction in expression from 4 to 10 mGy/h, and another increase from 10 to 100 mGy/h (phase 2). Only ubiquitin-conjugating enzyme E2–17 kDa (*Ube2*) displayed monotonic dose-dependent up-regulation (Fig. 1). Other genes such as Cu/Zn superoxide dismutase (*Sod*), H^+ transporting mitochondrial F1 complex ATP synthase alpha subunit 1 (*Atp5a1*), peroxisome proliferator-activated receptor gamma coactivator-related protein (*Ppar-g*), vitellogenin fused with superoxide dismutase (*Vtg1*), glycine *N*-methyltransferase (*Gnmt*) and ten-eleven translocation-2 (*Tet2*) showed more complex patterns of dose-response relationships. The majority of the genes tested were significantly (one-way ANOVA or Kruskal-Wallis test, $p < .05$) up-regulated by exposure to 100 mGy/h gamma radiation. Significant (one-way ANOVA or Kruskal-Wallis test, $p < .05$) increases in gene expression at lower gamma dose-rates were also observed for *Gst* (4 and 10 mGy/h), *Rev1* (4 mGy/h), *Triap* (40 mGy/h), *Ube2* (40 mGy/h) and *Atp5a1* (10 mGy/h). No significant change in *Sod*, *Vtg1* and *Gnmt* expression was identified.

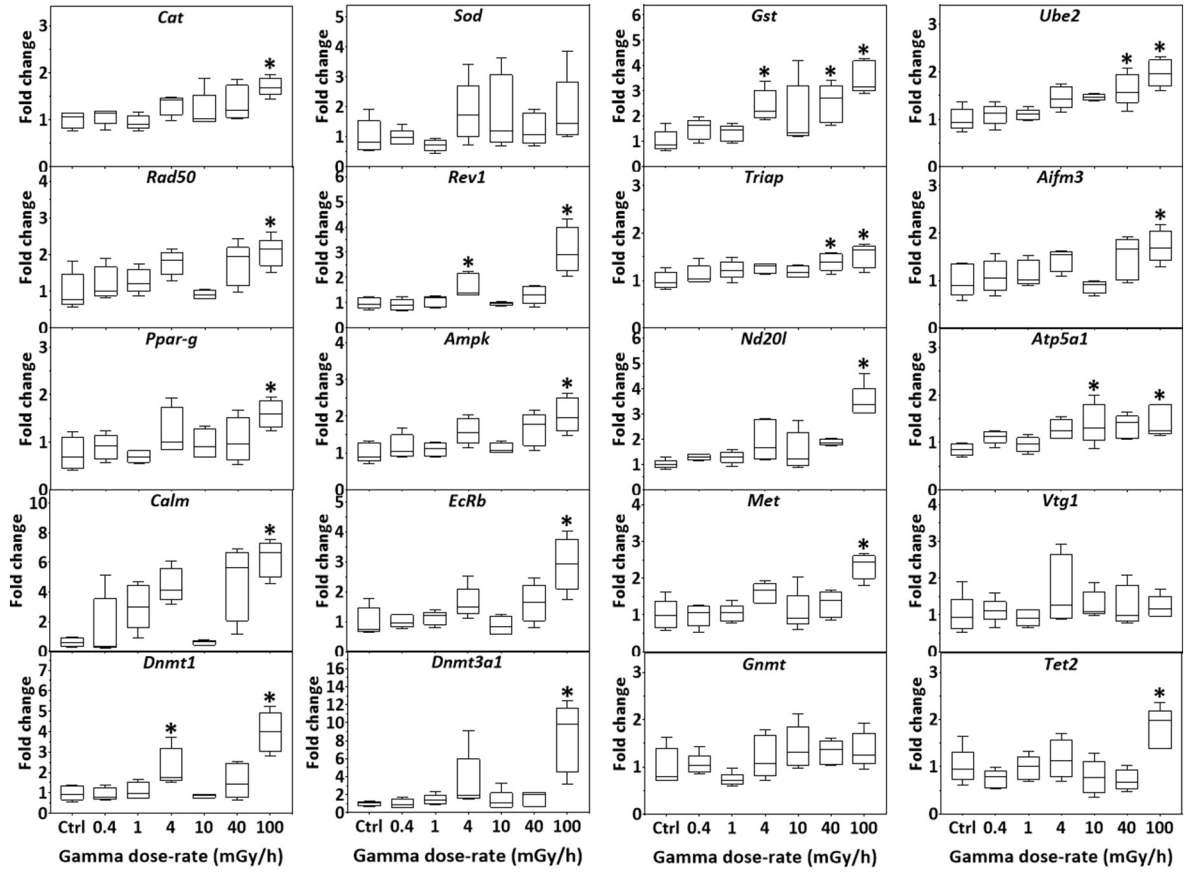

Fig. 1. Transcriptional responses in *Daphnia magna* after 8-day exposure to gamma radiation. *Gadph*: glyceraldehyde 3-phosphate dehydrogenase, *Cat*: catalase, *Sod*: Cu/Zn superoxide dismutase, *Gst*: glutathione s-transferase, *Ube2*: ubiquitin-conjugating enzyme E2–17 kDa, *Rad50*: DNA repair protein RAD50, *Rev1*: DNA directed polymerase REV1, *Triap*: TP53-regulated inhibitor of apoptosis 1, *Aifm3*: apoptosis-inducing factor 3, *Ppar-g*: peroxisome proliferator-activated receptor gamma coactivator-related protein, *Ampkα*: 5' -amp-activated protein kinase catalytic subunit alpha, *Nd-20l*: NADH dehydrogenase (ubiquinone) 20 kDa subunit, *Atp5a1*: H^+ transporting mitochondrial F1 complex ATP synthase alpha subunit 1, *Calm*: calmodulin, *EcRb*: ecdysone receptor B, *Met*: methoprene-tolerant, *Vtg1*: vitellogenin fused with superoxide dismutase, *Dnmt1*: DNA (cytosine-5)-methyltransferase 1, *Dnmt3a1*: DNA (cytosine-5)-methyltransferase 3A1, *Gnmt*: glycine *N*-methyltransferase, *Tet2*: ten-eleven translocation-2. * denotes significant difference (one-way ANOVA or Kruskal-Wallis test, $p < .05$) from the control.

1.13 Cellular responses

Dose-rate dependent formation of cellular ROS was observed in *D. magna* after 8-day exposure to gamma radiation, with 100 mGy/h gamma inducing significant (one-way ANOVA, $p < .05$) cellular (Fig. 2A) and LPO-related ROS (Fig. 2C), and both 40 and 100 mGy/h gamma inducing significant (one-way ANOVA, $p < .05$) mitochondrial ROS (Fig. 2B). After 8-day exposure, significant (one-way ANOVA, $p < .05$) induction of LPO was observed after exposure to 1, 4 and 100 mGy/h gamma (Fig. 2D), whereas significant (one-way ANOVA, $p < .05$) reduction in lipid storage was found at 4, 40 and 100 mGy/h (Fig. 2E). The ATP level in general decreased with increasing radiation dose-rates, with 100 mGy/h causing significant (one-way ANOVA, $p < .05$) reduction in whole-organism ATP content (Fig. 2F). The mitochondrial MMP was marginally affected (but not significantly so) by exposure to gamma radiation (Fig. 2G). Slight increases in apoptosis were also observed, however, the changes were not significant (Fig. 2H).

1.14 Tissue/Organ responses

After 14-day and 21-day exposure to gamma radiation, an apparent reduction in the number of follicles was observed in the *D. magna* ovary after exposure to 1 and 100 mGy/h gamma radiation (Fig. 3A & 3C). The embryos also had abnormal structures in *D. magna* exposed to higher dose-rates of the gamma radiation compared to 1 mGy/h and the control after both 14-day and 21-day exposure (Fig. 3A & 3C). In addition, the intestine microvilli structures were affected by gamma radiation with short and not well-arranged microvilli structures compared to control after 14-day and 21-day exposure (Fig. 3B & 3D).

1.15 Individual responses

No significant effects on survival, molting or ovulation frequency were observed after 21-day exposure, however there was a significant (one-way ANOVA, $p < .05$) reduction in cumulative fecundity observed after exposure to 1 and 100 mGy/h (Fig. 4A). The individual brood size was significantly (one-way ANOVA, $p < .05$) affected by exposure to 1 (brood 2), 10 (brood 1), and 100 mGy/h (broods 1 and 2) gamma radiation (Fig. 4A). The durations for completing broods 2, 3, and 4 were significantly (one-way ANOVA, $p < .05$) longer in *D. magna* exposed to 1 mGy/h radiation, whereas exposure to 100 mGy/h gamma displayed an apparent but non-significant reduction in the duration needed to complete all four broods compared to the control (Fig. 4B). The duration needed to complete brood 5 was not included in the comparison as not all daphnids completed brood 5 after 21 days.

1.16 Correlations

The Pearson correlation analysis identified positive correlations between cellular ROS formation, DNA damage response, mitochondrial electron transport chain activity, protein ubiquitination, calcium signaling, hormone receptor activities and DNA methylation, whereas these correlated negatively with fecundity and lipid storage (Appendix, Table A3). Principle component analysis (Fig. 5) showed that the majority of the endpoints were clustered with similar contributions to the

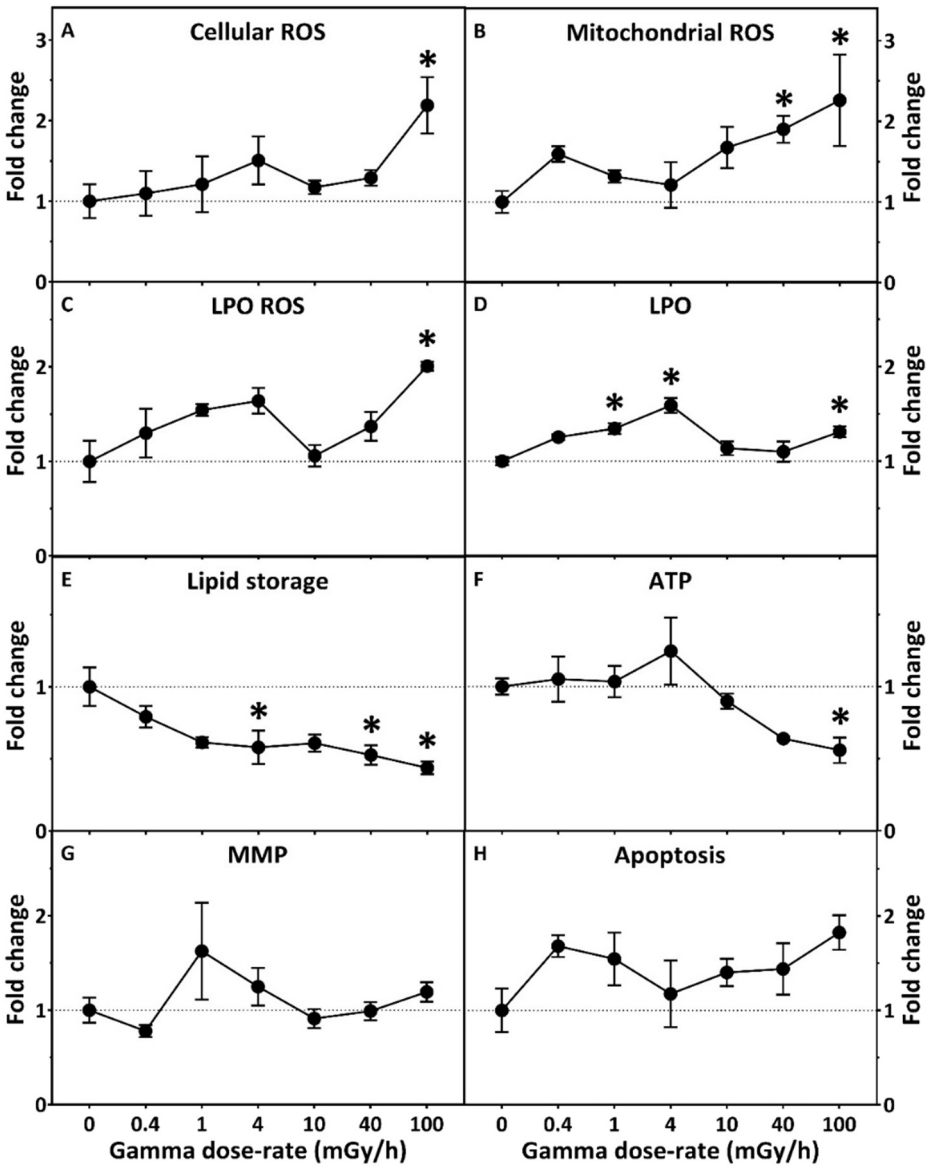

Fig. 2. Cellular (A), mitochondrial (B) and lipid peroxidation-related reactive oxygen species (ROS) formation (C), lipid peroxidation (D), lipid storage (E), ATP level (F), mitochondrial membrane potential (G) and apoptosis (H) in *Daphnia magna* after 8-day exposure to gamma radiation. Error bar indicates standard error of mean (SEM). * denotes significant difference (one-way ANOVA or Kruskal-Wallis test, $p < .05$) from the control.

variability of the data. Fecundity was negatively correlated with most of the endpoints, whereas mitochondrial ATP-related processes were not directly correlated with fecundity or other processes.

4. Discussion

The present study assessed the biological effects of gamma radiation on *D. magna* at the mGy/h dose-rate level, which is comparable with the measured dose-rates immediately after the nuclear accidents or radiation contamination events. For example, the highest dose-rate in fish after the Chernobyl accident was 633 μGy/h (Kryshev, 1998). In the Fukushima and Mayak accident areas, the radiation dose-rates were estimated to be 100–633 μGy/h (Battle et al., 2014) and 450 μGy/h (Kryshev et al., 1997), respectively. In Lake Karachay at Mayak PA in the Urals, the radiation dose-rate was estimated to be as high as 1 Gy/h (Cochran et al., 1993). Although water can act as a radiation shield, the radiation dose-rates tested in the present study could represent realistic exposure to aquatic organisms immediately after the nuclear events and in highly contaminated shallow ponds. It needs to be noted that the dose-rates used in this study represent extreme exposure scenarios and may not fully represent the current environmental dose-rates in some contaminated areas, such as that recently reported for the contaminated lakes at Chernobyl (Lerebours et al., 2018; Fuller et al., 2019; Goodman et al., 2019). At the mGy/h dose-rate level, gamma radiation caused adverse life-history effects on *D. magna* which were further characterized by alterations to numerous biomarkers representative of well-known toxicological pathways. Ionizing radiation at doses representative of contaminated sites may therefore potentially be hazardous to this keystone freshwater crustacean or other similar species. The mechanisms underlying gamma radiation-mediated reproductive effects will be discussed in detail in the following sections.

1.17 Mechanisms of action of gamma radiation

1.17.1 Induction of oxidative stress

Multiple lines of evidence from the present study suggest that oxidative stress was induced in *D. magna* following exposure to gamma radiation. Consistent induction of cellular, mitochondrial and LPO-related

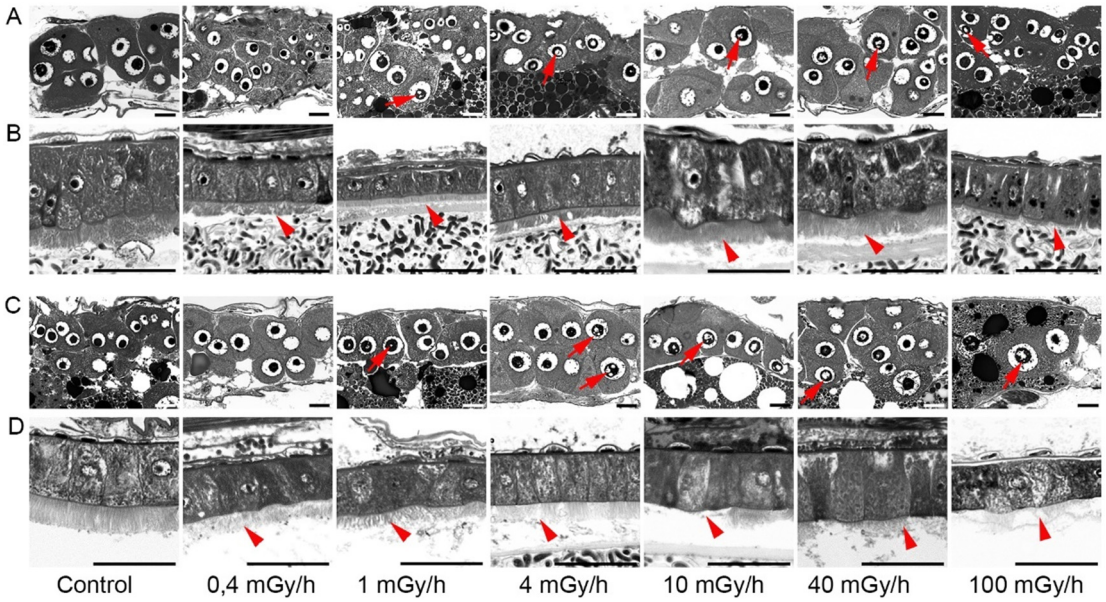

Fig. 3. Histological changes in *Daphnia magna* after 14-day (A & B) and 21-day (C & D) exposure to gamma radiation. A and C, Follicles. B and D Inside of guts. Arrows indicate abnormal oocytes production. Arrow heads indicate microvilli in the intestine that are short and not well-arranged after gamma irradiation compare to control. Scale bars: 25 μm.

ROS was detected using different probes, indicating cell-wide overproduction of ROS. Up-regulation of antioxidant genes such as *Cat* (scavenger of hydrogen peroxide) at 100 mGy/h and *Gst* (promoter of the antioxidant activity of glutathione) at as low as 4 mGy/h further indicated higher demand for ROS scavenging. By using a different exposure system (i.e., simpler medium composition and no algae feeding), an earlier study by Gomes et al. (2018) was able to detect significant cellular ROS formation in juvenile *D. magna* after 2-day exposure to gamma radiation dose-rates as low as 10.7 mGy/h, thus suggesting that different medium composition and/or the presence of green algae could influence the threshold for observable radiation effects.

Excessive ROS production can damage macromolecules such as DNA, lipids and proteins. Indirect evidence such as the up-regulation of two genes involved in different DNA repair pathways, *Rev1* (translesion synthesis of damaged DNA) (Hicks et al., 2010) and *Rad50* (double-strand break repair)(Lammens et al., 2011) at 100 mGy/h potentially suggests the presence of multiple types of DNA damage. Similar dose-rates of gamma radiation have been shown to induce DNA damage as early as 2 days after exposure, as directly measured by the single-cell gel electrophoresis (Comet) assay (Gomes et al., 2018). In addition, transcriptomic analysis in the same study also showed dose-rate dependent up-regulation of DNA repair genes such as *Rad50* by 42.9 mGy/h and double-strand break (DSB) repair protein MRE11 (*Mre11*) by as low as 1.1 mGy/h radiation, thus further supporting the induction of DNA damage by gamma radiation. It needs to be noted that gamma is known to cause DNA damage through direct energy deposition on DNA molecules, and/or through oxidation of DNA by ROS. It was not feasible to distinguish whether the DNA damage was caused by direct or indirect effects of gamma in the current study. However, in other crustaceans, a study by (Han et al., 2014) on the marine crustacean *Tigriopus japonicas* showed that exposure to sublethal doses of gamma radiation induced oxidative DNA damage. They also reported reproductive impairment and growth retardation as a result of radiation-induced DSBs. A similar study by (Won and Lee, 2014) reported that exposure to gamma radiation led to dose-dependent increase in mRNA expression of genes (e.g. Ku70, Ku80 and DNA-PK) involved in the non-homologous end joining (NHEJ) and DSB repair pathways in the copepod *Paracyclopina nana*.

A combination of LPO-related ROS formation and a non-monotonic increase in an LPO metabolite (i.e., malondialdehyde/MDA) identified in this study suggests that lipids were also damaged after 8-day exposure. Gamma radiation-mediated oxidative damage to lipids has

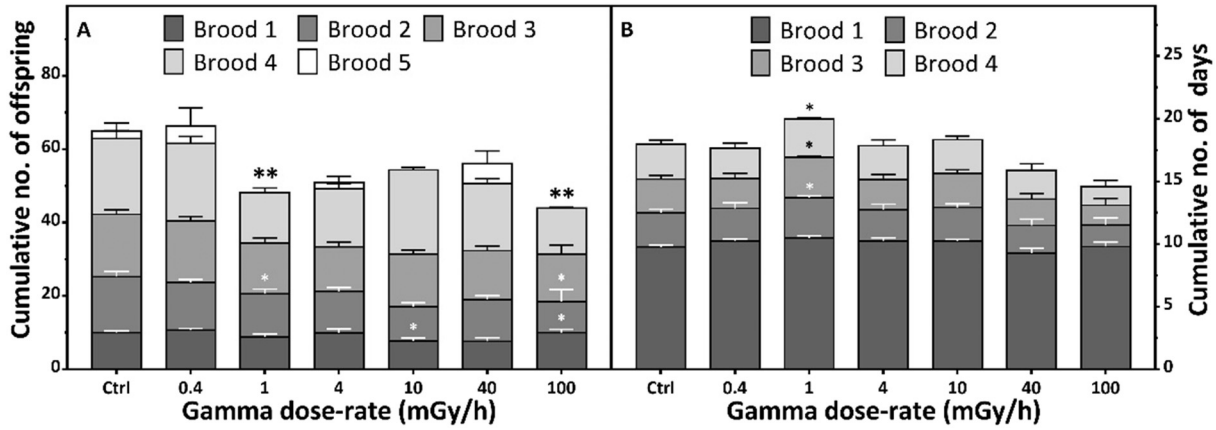

Fig. 4. Cumulative fecundity and brood sizes (A), and cumulative number of days to the completion of brood 1–4 (B) in adult *Daphnia magna* ($n = 5$–10) after 21-day exposure to gamma radiation. Error bars indicate standard error of mean (SEM). * denotes significant difference from the corresponding control in each brood. ** denotes significant difference (one-way ANOVA or Kruskal-Wallis test, $p < .05$) from the corresponding control in cumulative fecundity.

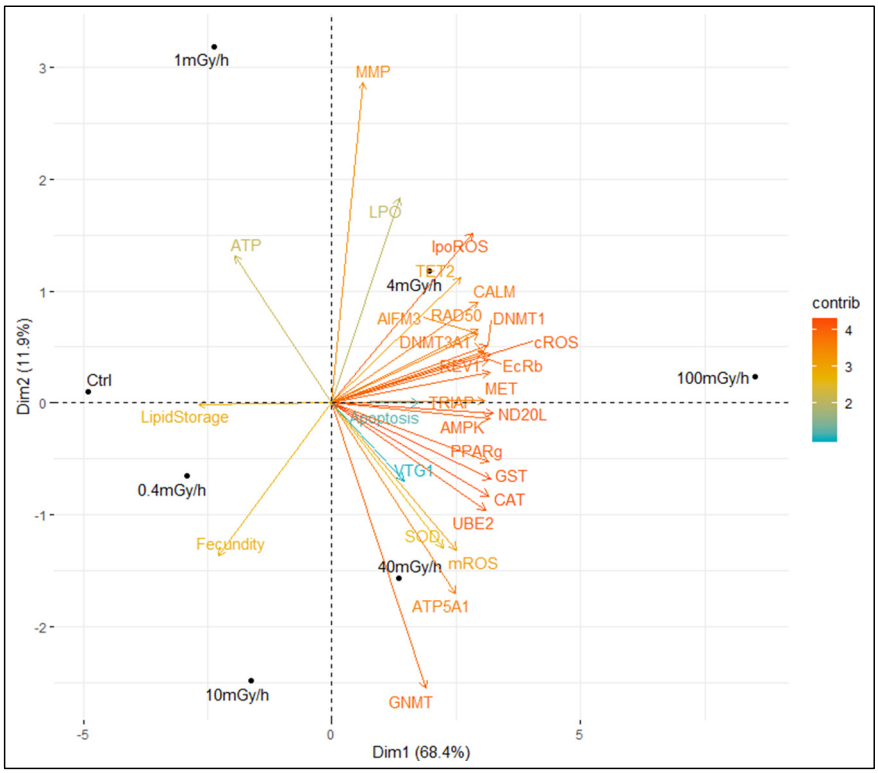

Fig. 5. Principle component analysis (PCA) of all test endpoints. Contrib: contribution to the variation; cROS: cellular reactive oxygen species (ROS), mROS: mitochondrial ROS, lpROS: lipid peroxidation-related ROS, LPO: lipid peroxidation, *Cat*: catalase, *Sod*: Cu/Zn superoxide dismutase, *Gst*: glutathione s-transferase, *Ube2*: ubiquitin-conjugating enzyme E2–17 kDa, *Rad50*: DNA repair protein RAD50, *Rev1*: DNA directed polymerase REV1, *Triap*: TP53-regulated inhibitor of apoptosis 1, *Aifm3*: apoptosis-inducing factor 3, *Ppar-g*: peroxisome proliferator-activated receptor gamma coactivator-related protein, *Ampkα*: 5' -amp-activated protein kinase catalytic subunit alpha, *Nd-20l*: NADH dehydrogenase (ubiquinone) 20 kDa subunit, *Atp5a1*: H^+ transporting mitochondrial F1 complex ATP synthase alpha subunit 1, *Calm*: calmodulin, *EcRb*: ecdysone receptor B, *Met*: methoprene-tolerant, *Vtg1*: vitellogenin fused with superoxide dismutase, *Dnmt1*: DNA (cytosine-5)-methyltransferase 1, *Dnmt3a1*: DNA (cytosine-5)-methyltransferase 3A1, *Gnmt*: glycine *N*-methyltransferase, *Tet2*: ten-eleven translocation-2.

previously been reported in *D. magna* after 24 h exposure to gamma radiation dose-rates as low as 10.7 mGy/h (Gomes et al., 2018).

The dose-rate dependent up-regulation of *Ube2*, a gene involved in protein degradation (Nandi et al., 2006), provided indirect evidence to support radiation-mediated oxidative protein damage, excessive ROS is known to cause protein oxidation (Berlett and Stadtman, 1997). The oxidized proteins are degraded by proteasomes where *Ube2* plays an important role (Jung et al., 2014). Increased expression of *Ube2* may thus indicate elevated demand for elimination of damaged proteins. Nevertheless, this toxicity pathway needs further investigation through direct measurement of protein oxidation.

1.17.2 Depletion of cellular energy

On the basis of the supporting evidence from the present study, it is proposed that mitochondrial ATP production was disrupted by gamma radiation. The *Ampk* gene, a sensor and master regulator of cellular energy status (Mihaylova and Shaw, 2011), was up-regulated at 100 mGy/h, indicating a cell-wide energy shortage. This gene up-regulation was in line with the whole-organism ATP level which in general showed dose-rate dependent reduction. Additional evidence, such as the up-regulation of *Nd20l*, a gene involved in the mitochondrial electron transport complex I (Foriel et al., 2019), and *Atp5a1*, a gene encoding the mitochondrial ATP synthase (Bernardi et al., 2015), suggests demand for elevated mitochondrial electron transport chain activity as a compensatory mechanism to ATP depletion. Unexpectedly, the mitochondrial MMP did not show significant changes compared to the control, indicating that gamma radiation likely affected ATP production through a mitochondrial membrane-independent toxicity pathway, such as direct inference with the ETC protein complexes (reviewed in Kam and Banati (2013)). Mitochondrial dysfunction is considered a main cause of increased endogenous ROS production and genomic instability after exposure to ionizing radiation (Yoshida et al., 2012; Szumiel, 2015). In addition, it is previously suggested that the mitochondrial ultrastructure, which is pivotal to all physiological processes in the mitochondria, can be affected by ROS (Brandt et al., 2017; Raffa et al., 2017; Ježek et al., 2018). Although mitochondrial ultrastructure was not included as an endpoint in this study, it is interesting to include this in future studies as an additional observation for radiation-induced mitochondrial dysfunction.

1.17.3 Perturbation to lipid homeostasis

It is widely known that oxidative stressors can affect lipid homeostasis by causing lipid peroxidation in organisms (Niki, 2008). Interestingly, results from the present study support the suggestion that exposure to gamma radiation affected lipid homeostasis and led to a dose-rate dependent decrease in neutral lipid storage in *D. magna*. In addition, dose-rate dependent up-regulation of *Ppar-g*, a key nuclear receptor involved in the regulation of fatty acid storage (Varga et al., 2011; Jordao et al., 2016), also indicated increased demand for lipid storage potentially due to oxidative lipid damage, and elevated consumption of lipids for maintaining plasma membrane integrity and use of energy in cellular defense mechanisms (Olzmann and Carvalho, 2019).

1.17.4 Activation of apoptotic cell death

Apoptosis, which is activated in response to oxidative stress or direct DNA damage, eliminates damaged cells and protects organisms from genomic instability and mutations (Elmore, 2007). Apoptosis has been

indicated as a key downstream effect of oxidative stress in crustaceans (Menze et al., 2010), and although not statistically significant, results from the TUNEL assay indicated a trend of increasing apoptotic cell death with an increasing radiation dose-rate in *D. magna*. Additional evidence such as the up-regulation of the mitochondrial apoptosis initiator *Aifm3*, and the apoptosis inhibitor *Triap*, further supports that apoptosis is induced in *D. magna* after exposure to gamma radiation. Ionizing radiation and resultant ROS are known to induce mitochondrial apoptotic signaling, which is the intrinsic pathway of apoptosis in mammalian cells (Ferri and Kroemer, 2001). Evidence for this same pathway is limited for invertebrates (Menze et al., 2010), albeit abnormal mitochondria have been observed in apoptotic bodies present in the Norway lobster *Nephrops norvegicus* after exposure to 0.5 Gy Co-60 gamma radiation (Lyng et al., 2003). Induction of apoptosis has also been shown in *Drosophila* at a high (40 Gy) total dose of ionizing radiation (Shim et al., 2014) and in the crab *Ucides cordatus* when exposed to other radiation sources such as UVB/UVC (Miguel et al., 2007).

1.17.5 Augment of calcium influx

Calcium is an important nutrient and a central messenger ion involved in diverse types of biological processes. The present study showed that *Calm*, a master sensor and regulator of intracellular calcium (Faas et al., 2011), was highly up-regulated in a non-monotonic manner by exposure to gamma radiation. Similar non-monotonic up-regulation of *Calm* was also reported for *D. magna* after 48 h exposure to 0.41–106 mGy/h gamma radiation (Gomes et al., 2018). Up-regulation of *Calm* possibly indicates increased intracellular calcium influx, which is considered pivotal to many physiological processes, such as maintaining the mitochondrial membrane potential (Rottenberg and Scarpa, 1974), apoptosis (Smaili et al., 2000), neurotransmission (Sudhof, 2012) and crustacean molting (Greenaway, 1985). Abnormal calcium signaling may thus lead to various types of physiological dysfunctions.

1.17.6 Disruption of hormone receptor signaling

Hormone receptors are key for endocrine regulation of various physiological processes. Interestingly, two hormone receptors, *EcRb* and *Met* displayed non-monotonic up-regulation in *D. magna* by exposure to gamma radiation. The *EcRb* gene is one of the main upstream regulators of molting and development in arthropods (Schubiger et al., 1998; Song et al., 2017), whereas the *Met* gene is mainly responsible for sex determination and reproduction (Miyakawa et al., 2013; Zou et al., 2013). Up-regulation of these hormone receptors may indicate disruption of normal endocrine functions after radiation exposure. The abnormal regulation of the hormone receptors may potentially be linked to enhanced calcium signaling identified in the present study, as this intracellular signaling molecule has a key role in hormone synthesis and signaling in invertebrates(Smith and Gilbert, 1986; Chang and Mykles, 2011).

1.17.7 Enhancement of DNA methylation

DNA methylation is an important mechanism employed to regulate gene transcription. Genes involved in the one-carbon metabolism pathway to regulate DNA methylation, such as *Dnmt1* (maintenance of DNA methylation), *Dnmt3a1* (de novo DNA methylation) and *Tet2* (regulation of DNA demethylation) (Mentch and Locasale, 2016), were found to be significantly up-regulated by exposure to gamma radiation at 100 mGy/h. Gamma radiation has been reported to alter DNA methylation and cause transgenerational effects in *D. magna* (Trijau et al., 2018). Enhanced DNA methylation in humans is normally linked to gene silencing, whereas in daphnids, a positive correlation between increased gene expression and higher methylation has been shown (Kvist et al., 2018). Formation of ROS may also lead to hypermethylation (Lim et al., 2008), potentially explaining the up-regulation of methylation linked genes (i.e., *Dnmt1*, *Dnmt3a1*). If key genes involved in the repair mechanisms in response to ionizing radiation, such as the antioxidant genes or DNA repair genes were silenced by DNA methylation, damage to the organism may accumulate and detrimental effects such as mutation and tumorigenesis may be promoted (Lahtz and Pfeifer, 2011; Guo et al., 2015). Furthermore, in relation to the one-carbon metabolism, genomic imprinting is strongly correlated to ROS and methylation (Hoffman, 2011; Menezo et al., 2011) where imprints are first erased and then re-established leading to effects on the quality of the gametes (reviewed in Menezo et al. (2016)).

1.18 Effects of gamma radiation on apical endpoints

4.1.1. Ovary structure and oogenesis

The histopathological analysis in the present study showed that both the ovary structure and oocyte development in *D. magna* were impaired after exposure to gamma radiation, as evidenced from a reduced number of intact follicles and abnormal morphology in oocytes. Ionizing radiation has been documented to affect oogenesis through induction of cell cycle arrest, apoptosis and developmental defects in invertebrates such as *Drosophila* (Shim et al., 2014). Impaired oogenesis is also considered a direct consequence of oxidative stress in invertebrates (Perkins et al., 2016). Microvilli in the intestine were damaged after gamma radiation treatment in *Daphnia* and similar effect was also observed in the human intestine system after radiation treatment (Jalili-Firoozinezhad et al., 2018). Since the microvilli significantly increases the surfaces of the gut cells, damage may lead to reduced efficiency of nutrient uptake (Walton et al., 2016), thus affecting energy metabolism (Lange, 2002).

4.1.2. Reproductive cycle and fecundity

Gamma radiation has been reported to affect fecundity in *D. magna* at mGy/h dose-rate levels (Gilbin et al., 2008; Parisot et al., 2015; Sarapultseva and Dubrova, 2016). Results from the present study also indicate that chronic exposure to gamma radiation reduced the total number of offspring in *D. magna* without affecting survival, molting or ovulation frequency. Interestingly, a non-monotonic reduction in reproductive output was observed, with both low (1 mGy/h) and high (100 mGy/h) test dose-rates causing significantly reduced cumulative fecundity. Additional observations on the total days for completing each brood suggested that the causes of reduced fecundity may be dissimilar between 1 and 100 mGy/h. It seems that at 1 mGy/h, reduction in cumulative fecundity was mainly caused by radiation-mediated reproduction delay in *D. magna*, as clearly supported by the significantly higher number of days required to complete broods 2–4. Delayed reproduction in *D. magna* was reported after exposure to an ionizing radiation dose-rate of 15 mGy/h (Alonzo et al., 2008a; Alonzo et al., 2008b) and in the marine copepod *Paracyclopina nana* after exposure to a total dose of 10 Gy (Won and Lee, 2014). On the contrary, exposure to 100 mGy/h slightly accelerated the reproduction cycles with reduced total number of offspring mainly attributed to compromised size of each brood. A similar non-monotonic adverse effect of ionizing radiation has also been documented by Parisot et al. (2015) where chronic (23-day) exposure to 0.007 and 35.4 mGy/h external gamma radiation emitted from a Cs-137 source significantly decreased the cumulative fecundity in *D. magna*, whereas the reproductive output remained relatively unchanged at the intermediate dose-rates. Interestingly, Goodman et al. (2019) also noted a non-monotonic pattern in *D. magna* offspring production from isofemale lines representing 38 genotypes from eight lakes within the Chernobyl Exclusion Zone (corresponding to dose-rates between 0.1 and 181.2 μGy/h), with the first peak in offspring production from animals historically exposed to 0.2 μGy/h and a second peak for animals historically exposed to 115.7 μGy/h. Whereas it may be challenging to draw direct parallels between highly controlled laboratory exposures using naïve animals versus trials using site adapted experienced animals, nonetheless, these findings collectively suggest that the mechanisms of how gamma radiation affect reproduction may be highly dose-rate dependent.

1.19 Evidence-based toxicity pathway network assembly

A hypothetical network of toxicity pathways on ionizing radiation-mediated reproductive effects was assembled based on the supporting evidence from the present study and literature (Fig. 6) as one of the novelties in the present study. Five major pathways were included in the network: 1) ROS formation leading to reduced lipid storage associated reproductive malfunction; 2) ROS formation leading to mitochondrial dysfunction associated reproductive malfunction; 3) ROS formation leading to abnormal calcium signaling associated reproductive decline; 4) ROS formation leading to DNA damage and apoptosis associated reproductive reduction; 5) ROS formation leading to DNA methylation associated reproductive effects. It has been widely accepted that ionizing radiation can induce excessive ROS through ionization and excitation of water in organisms (Azzam et al., 2012). Macromolecules such as DNA, lipid and protein are considered the major targets of ROS in most species (Pacifici and Davies, 1991). Oxidative DNA damage is a direct consequence of ROS-induced DNA damage which can further activate programmed cell death such as apoptosis to eliminate damage cells (Redza-Dutordoir and Averill-Bates, 2016). Apoptosis in the ovary can affect the formation of follicles and result in follicular atresia which ultimately affect the development of oocytes in the ovary (Devine et al., 2012). Lipid peroxidation is also a well-known consequence of excessive ROS formation (Benzie, 1996). Based on the current findings, it is suspected that lipid peroxidation may increase lipid degradation thus reduce lipid storage. Reduced fatty acid oxidation as a result of lipid degradation may reduce lipid-based ATP production (Houten et al., 2016). It is also well-known that ROS can cause mitochondrial dysfunction through modulating the mitochondrial membrane thus impair mitochondrial oxidative phosphorylation (Zorov et al., 2006), albeit this was not confirm by the current data. Another hypothesis is that the mitochondrial oxidative phosphorylation is reduced to minimize the production of endogenous ROS in the mitochondria (Zorov et al., 2006). Both types of alterations can lead to reduced ATP production which has also been observed in the present study. There are also several hypothetical pathways with less supporting evidence from the literature, such as gut microvilli damage associated energy depletion, abnormal calcium signaling associated modulation to the endocrine systems, and altered epigenetic regulation of gene expression (Fig. 6), but they are clearly worthy of further considerations in future studies.

1.20 Adverse outcome pathway development

On the basis of the toxicity pathway network, three AOPs (Fig. 7) were developed based on the hypothetical toxicity pathway network and submitted to the public AOP repository AOPWiki (https://aopwiki.org/): 1) Excessive ROS production leading to DNA damage-mediated reproductive dysfunction (AOP #216); 2) Excessive ROS production leading to ATP depletion-mediated reproductive failure (AOP #238); 3) Excessive ROS production leading to lipid peroxidation-associated reproduction decrease (AOP#311). These AOPs are potentially applicable to most of the oxidative stressors (i.e., radiation, metals and organics that cause oxidative stress) which commonly induce ROS as an MIE. The taxonomic applicability will cover a wide range of aquatic species who produce oocyte for reproduction, such as crustaceans, insects and fish. A list of methods for detecting the KEs in the AOPs has been suggested in Appendix (Table A4). These novel AOPs represent the world's first AOPs for non-chemical stressors and invertebrates which will be further developed for better mechanistic understanding of radiation effects on aquatic organisms and improved radiation safety evaluation. As AOPs are living documents, these AOPs will be further refined with the accumulation of supporting evidence and improvement of analytical method for KE quantification.

5. Conclusions

The present study is an integrative toxicological effect assessment for understanding the potential hazards of a high-energy low-dose ionizing radiation across multiple levels of biological organization in *D. magna*. Results obtained clearly suggest that multiple toxicity pathways were potentially involved in gamma radiation-mediated reproductive effects, such as the DNA damage-oocyte apoptosis pathway, lipid peroxidation-ATP depletion pathway, calcium influx-endocrine disruption pathway and DNA hypermethylation pathway. These pathways were assembled into a toxicity pathway network and can serve as a knowledge foundation for mechanistic understanding of ionizing radiation-mediated reproductive effects on aquatic organisms. Two conceptual adverse outcome pathways (AOPs) were developed based on the supporting evidence from the present study and represent the world's first AOPs for next generation environmental hazard and risk assessment of ionizing radiation and associated radionuclides. Future

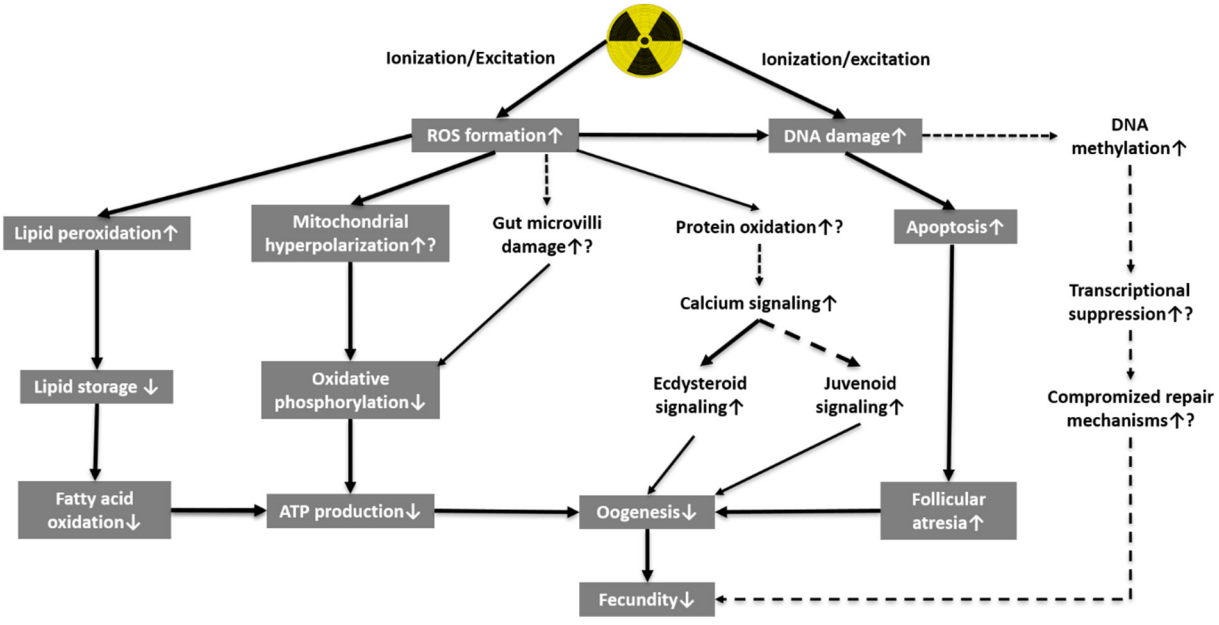

Fig. 6. Proposed major toxicity pathways describing gamma radiation-mediated reproductive effects in *Daphnia magna*. Shadowed terms are considered key events in the conceptual adverse outcome pathways.

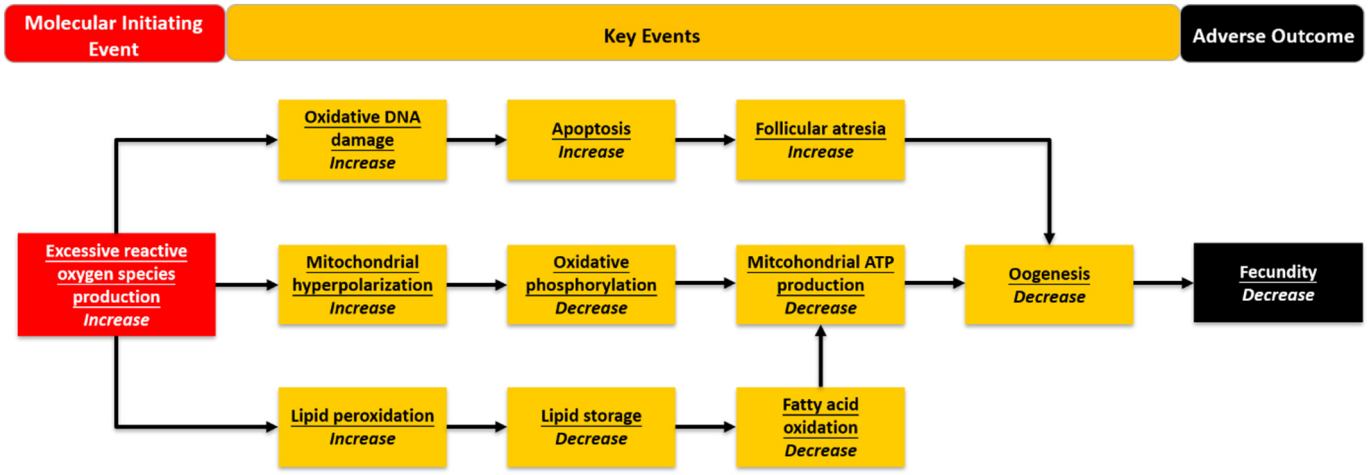

Fig. 7. A network of adverse outcome pathways (AOPs) on oxidative stressor-mediated reproductive effects in aquatic organisms. The network consists of three linear AOPs which have been submitted to the AOP repository AOPWiki (https://aopwiki.org/, AOP #216, #238 and #311).

work will also focus on the development of quantitative models (quantitative AOPs/qAOPs) for predicting the effects of oxidative stressors in aquatic organisms.

Declaration of Competing Interests.

The authors declare that they have no known competing financial interests or personal relationships that could have appeared to influence the work reported in this paper.

Acknowledgement

The present work was funded by the Research Council of Norway through the Centre of Excellence (CoE) project "Centre for Environmental Radioactivity (CERAD, project No. 223268)", and supported by the NIVA Computational Toxicology Program (NCTP, https://www.niva.no/en/projectweb/nctp). The authors also acknowledge the technical support from Tania Gomes (NIVA), David Eidsvoll (NIVA), Ole Christian Lind (NMBU), Leif Lindeman (NMBU), Jorke Kamstra (NMBU) and Jana Asselman (Ghent University, Belgium).

Appendix A. Supplementary data

Supplementary data to this article can be found online at https://doi.org/10.1016/j.scitotenv.2019.135912.

References

Alonzo, F., Gilbin, R., Zeman, F.A., Garnier-Laplace, J., 2008a. Increased effects of internal alpha irradiation in Daphnia magna after chronic exposure over three successive generations. Aquat. Toxicol. 87, 146–156.

Alonzo, F., Hertel-Aas, T., Gilek, M., Gilbin, R., Oughton, D.H., Garnier-Laplace, J., 2008b. Modelling the propagation of effects of chronic exposure to ionising radiation from individuals to populations. J. Environ. Radioact. 99, 1464–1473.

Ankley, G.T., Bennett, R.S., Erickson, R.J., Hoff, D.J., Hornung, M.W., Johnson, R.D., Mount, D.R., Nichols, J.W., Russom, C.L., Schmieder, P.K., Serrrano, J.A., Tietge, J.E., Villeneuve, D.L., 2010. Adverse outcome pathways: a conceptual framework to support ecotoxicology research and risk assessment. Environ. Toxicol. Chem. 29, 730–741.

Azzam, E.I., Jay-Gerin, J.P., Pain, D., 2012. Ionizing radiation-induced metabolic oxidative stress and prolonged cell injury. Cancer Lett. 327, 48–60.

Barata, C., Varo, I., Navarro, J.C., Arun, S., Porte, C., 2005. Antioxidant enzyme activities and lipid peroxidation in the freshwater cladoceran Daphnia magna exposed to redox cycling compounds. Comp Biochem Physiol C Toxicol Pharmacol 140, 175–186.

Battle, J.V.I., Aono, T., Brown, J.E., Hosseini, A., Gamier-Laplace, J., Sazykina, T., Steenhuisen, F., Strand, P., 2014. The impact of the Fukushima nuclear accident on marine biota: retrospective assessment of the first year and perspectives. Sci. Total Environ. 487, 143–153.

Benzie, I.F.F., 1996. Lipid peroxidation: a review of causes, consequences, measurement and dietary influences. Int. J. Food Sci. Nutr. 47, 233–261.

Beresford, N.A., Copplestone, D., 2011. Effects of ionizing radiation on wildlife: what knowledge have we gained between the Chernobyl and Fukushima accidents? Integr. Environ. Assess. Manag. 7, 371–373.

Berlett, B.S., Stadtman, E.R., 1997. Protein oxidation in aging, disease, and oxidative stress. J. Biol. Chem. 272, 20313–20316.

Bernardi, P., Di Lisa, F., Fogolari, F., Lippe, G., 2015. From ATP to PTP and back: a dual function for the mitochondrial ATP synthase. Circ. Res. 116, 1850–1862.

Bjerke, H., Hetland, P.O., 2014. Dosimetri ved FIGARO gammaanlegget ved NMBU, Ås. Målerapport fra oppmåling av doseraten i strålefeltet fra kobolt-60. NRPA Technical Document Series 2. Norwegian Radiation Protection Authority, Oslo, Norway.

Brandt, T., Mourier, A., Tain, L.S., Partridge, L., Larsson, N.-G., Kühlbrandt, W., 2017. Changes of mitochondrial ultrastructure and function during ageing in mice and drosophila. eLife 6, e24662.

Burns, C.W., Schallenberg, M., 1996. Relative impacts of copepods, cladocerans and nutrients on the microbial food web of a mesotrophic lake. J. Plankton Res. 18, 683–714.

Cauchie, H.M., Thys, I., Hoffmann, L., Thome, J.P., 2000. In situ versus laboratory estimations of length-weight regression and growth rate of *Daphnia magna* (Branchiopoda, Anomopoda) from an aerated waste stabilization pond. Hydrobiologia 421, 47–59.

Chang, E.S., Mykles, D.L., 2011. Regulation of crustacean molting: a review and our perspectives. Gen. Comp. Endocrinol. 172, 323–330.

Cochran, T.B., Robert Standish Norris, a, Suokko, K.L., 1993. Radioactive contamination at Chelyabinsk-65, Russia. Annu. Rev. Energy Environ. 18, 507–528.

Covich, A.P., Palmer, M.A., Crowl, T.A., 1999. The role of benthic invertebrate species in freshwater ecosystems: zoobenthic species influence energy flows and nutrient cycling. BioScience 49, 119–127.

Dallas, L.J., Keith-Roach, M., Lyons, B.P., Jha, A.N., 2012. Assessing the impact of ionizing radiation on aquatic invertebrates: a critical review. Radiat. Res. 177, 693–716.

Devine, P.J., Perreault, S.D., Luderer, U., 2012. Roles of reactive oxygen species and antioxidants in ovarian toxicity. Biol. Reprod. 86, 27.

Elmore, S., 2007. Apoptosis: a review of programmed cell death. Toxicol. Pathol. 35, 495–516.

Faas, G.C., Raghavachari, S., Lisman, J.E., Mody, I., 2011. Calmodulin as a direct detector of Ca2+ signals. Nat. Neurosci. 14, 301–304.

Fay, K.A., Villeneuve, D.L., Lalone, C.A., Song, Y., Tollefsen, K.E., Ankley, G.T., 2017. Practical approaches to adverse outcome pathway development and weight-of-evidence evaluation as illustrated by ecotoxicological case studies. Environ. Toxicol. Chem. 36, 1429–1449.

Ferri, K.F., Kroemer, G., 2001. Organelle-specific initiation of cell death pathways. Nat. Cell Biol. 3, E255–E263.

Foriel, S., Renkema, G.H., Lasarzewski, Y., Berkhout, J., Rodenburg, R.J., Smeitink, J.A.M., Beyrath, J., Schenck, A., 2019. A drosophila mitochondrial complex I deficiency phenotype array. Front. Genet. 10, 245.

Fuller, N., Lerebours, A., Smith, J.T., Ford, A.T., 2015. The biological effects of ionising radiation on crustaceans: a review. Aquat. Toxicol. 167, 55–67.

Fuller, N., Smith, J.T., Nagorskaya, L.L., Gudkov, D.I., Ford, A.T., 2017. Does Chernobyl-derived radiation impact the developmental stability of Asellus aquaticus 30 years on? Sci. Total Environ. 576, 242–250.

Fuller, N., Ford, A.T., Lerebours, A., Gudkov, D.I., Nagorskaya, L.L., Smith, J.T., 2019. Chronic radiation exposure at Chernobyl shows no effect on genetic diversity in the freshwater crustacean, Asellus aquaticus thirty years on. Ecology and Evolution 9, 10135–10144.

Gilbin, R., Alonzo, F., Garnier-Laplace, J., 2008. Effects of chronic external gamma irradiation on growth and reproductive success of Daphnia magna. J. Environ. Radioact. 99, 134–145.

Gomes, T., Song, Y., Brede, D.A., Xie, L., Gutzkow, K.B., Salbu, B., Tollefsen, K.E., 2018. Gamma radiation induces dose-dependent oxidative stress and transcriptional alterations in the freshwater crustacean daphnia magna. Sci. Total Environ. 628–629, 206–216.

Goodman, J., Copplestone, D., Laptev, G.V., Gashchak, S., Auld, S.K.J.R., 2019. Variation in chronic radiation exposure does not drive life history divergence among daphnia populations across the Chernobyl exclusion zone. Ecology and Evolution 9, 2640–2650.

Greenaway, P., 1985. Calcium balance and molting in the Crustacea. Biol. Rev. Camb. Philos. Soc. 60, 425–454.
Guo, Y., Yu, S.W., Zhang, C.Y., Kong, A.N.T., 2015. Epigenetic regulation of Keap1-Nrf2 signaling. Free Radic. Biol. Med. 88, 337–349.
Han, J., Won, E.-J., Lee, B.-Y., Hwang, U.-K., Kim, I.-C., Yim, J.H., Leung, K.M.Y., Lee, Y.S., Lee, J.-S., 2014. Gamma rays induce DNA damage and oxidative stress associated with impaired growth and reproduction in the copepod Tigriopus japonicus. Aquat. Toxicol. 152, 264–272.
Hicks, J.K., Chute, C.L., Paulsen, M.T., Ragland, R.L., Howlett, N.G., Gueranger, Q., Glover, T.W., Canman, C.E., 2010. Differential roles for DNA polymerases eta, zeta, and REV1 in lesion bypass of intrastrand versus interstrand DNA cross-links. Mol. Cell. Biol. 30, 1217–1230.
Hoffman, M., 2011. Hypothesis: Hyperhomocysteinemia is an indicator of oxidant stress. Med. Hypotheses 77, 1088–1093.
Houten, S.M., Violante, S., Ventura, F.V., Wanders, R.J., 2016. The biochemistry and physiology of mitochondrial fatty acid beta-oxidation and its genetic disorders. Annu. Rev. Physiol. 78, 23–44.
Ianora, A., Miralto, A., Poulet, S.A., Carotenuto, Y., Buttino, I., Romano, G., Casotti, R., Pohnert, G., Wichard, T., Colucci-D'Amato, L., Terrazzano, G., Smetacek, V., 2004. Aldehyde suppression of copepod recruitment in blooms of a ubiquitous planktonic diatom. Nature 429, 403–407.
Jalili-Firoozinezhad, S., Prantil-Baun, R., Jiang, A., Potla, R., Mammoto, T., Weaver, J.C., Ferrante, T.C., Kim, H.J., Cabral, J.M.S., Levy, O., Ingber, D.E., 2018. Modeling radiation injury-induced cell death and countermeasure drug responses in a human gut-on-a-Chip. Cell Death Dis. 9, 223.
Janero, D.R., 1990. Malondialdehyde and thiobarbituric acid-reactivity as diagnostic indexes of lipid-peroxidation and peroxidative tissue-injury. Free Radic. Biol. Med. 9, 515–540.
Ježek, J., Cooper, K.F., Strich, R., 2018. Reactive oxygen species and mitochondrial dynamics: the yin and yang of mitochondrial dysfunction and cancer progression. Antioxidants (Basel, Switzerland) 7, 13.
Jordao, R., Casas, J., Fabrias, G., Campos, B., Pina, B., Lemos, M.F., Soares, A.M., Tauler, R., Barata, C., 2015. Obesogens beyond vertebrates: lipid perturbation by Tributyltin in the crustacean Daphnia magna. Environ. Health Perspect. 123, 813–819.
Jordao, R., Campos, B., Pina, B., Tauler, R., Soares, A.M.V.M., Barata, C., 2016. Mechanisms of action of compounds that enhance storage lipid accumulation in *Daphnia magna*. Environmental Science & Technology 50, 13565–13573.
Jung, T., Hohn, A., Grune, T., 2014. The proteasome and the degradation of oxidized proteins: part II - protein oxidation and proteasomal degradation. Redox Biol. 2, 99–104.
Kam, W.W., Banati, R.B., 2013. Effects of ionizing radiation on mitochondria. Free Radic. Biol. Med. 65, 607–619.
Kryshev, A.I., 1998. Modelling the accidental radioactive contamination and assessment of doses to biota in the Chernobyl NPP's cooling pond. Proceedings of the Topical Meeting of International Union of Radioecologists, pp. 32–38.
Kryshev, I.I., Romanov, G.N., Isaeva, L.N., Kholina, Y.B., 1997. Radioecological state of lakes in the southern Ural impacted by radioactivity release of the 1957 radiation accident. J. Environ. Radioact. 34, 223–235.
Kvist, J., Goncalves Athanasio, C., Shams Solari, O., Brown, J.B., Colbourne, J.K., Pfrender, M.E., Mirbahai, L., 2018. Pattern of DNA methylation in daphnia: evolutionary perspective. Genome Biol Evol 10, 1988–2007.
Lahtz, C., Pfeifer, G.P., 2011. Epigenetic changes of DNA repair genes in cancer. J. Mol. Cell Biol. 3, 51–58.
Lammens, K., Bemeleit, D.J., Mockel, C., Clausing, E., Schele, A., Hartung, S., Schiller, C.B., Lucas, M., Angermuller, C., Soding, J., Strasser, K., Hopfner, K.P., 2011. The Mre11: Rad50 structure shows an ATP-dependent molecular clamp in DNA double-strand break repair. Cell 145, 54–66.
Lange, K., 2002. Role of microvillar cell surfaces in the regulation of glucose uptake and organization of energy metabolism. Am. J. Phys. Cell Phys. 282, C1–C26.
Lerebours, A., Gudkov, D., Nagorskaya, L., Kaglyan, A., Rizewski, V., Leshchenko, A., Bailey, E.H., Bakir, A., Ovsyanikova, S., Laptev, G., Smith, J.T., 2018. Impact of environmental radiation on the health and reproductive status of fish from Chernobyl. Environ Sci Technol 52, 9442–9450.
Lim, S.O., Gu, J.M., Kim, M.S., Kim, H.S., Park, Y.N., Park, C.K., Cho, J.W., Park, Y.M., Jung, G., 2008. Epigenetic changes induced by reactive oxygen species in hepatocellular carcinoma: methylation of the E-cadherin promoter. Gastroenterology 135, 2128–2140 (2140 e2121-2128).
Lind, O.C., Helen Oughton, D., Salbu, B., 2019. The NMBU FIGARO low dose irradiation facility. Int. J. Radiat. Biol. 95, 76–81.
Lyng, F.M., Olwell, P., Ni Shuilleabhain, S., Mulford, A., Austin, B., Seymour, C., 2003. A comparative study of the effect of low doses of ionising radiation on primary cultures from rainbow trout, Oncorhynchus mykiss, and Dublin Bay prawn, Nephrops norvegicus. Protection of the Environment from Ionising Radiation–The Development and Application of a System of Radiation Protection for the Environment. International Atomic Energy Agency, Vienna, pp. 25–31.
Menezo, Y., Mares, P., Cohen, M., Brack, M., Viville, S., Elder, K., 2011. Autism, imprinting and epigenetic disorders: a metabolic syndrome linked to anomalies in homocysteine recycling starting in early life?? J. Assist. Reprod. Genet. 28, 1143–1145.
Menezo, Y.J., Silvestris, E., Dale, B., Elder, K., 2016. Oxidative stress and alterations in DNA methylation: two sides of the same coin in reproduction. Reprod. BioMed. Online 33, 668–683.
Mentch, S.J., Locasale, J.W., 2016. One-carbon metabolism and epigenetics: understanding the specificity. Diet, Sulfur Amino Acids, and Health Span 1363, 91–98.
Menze, M.A., Fortner, G., Nag, S., Hand, S.C., 2010. Mechanisms of apoptosis in Crustacea: what conditions induce versus suppress cell death? Apoptosis 15, 293–312.
Miguel, N.C., Wajsenzon, I.J., Takiya, C.M., de Andrade, L.R., Tortelote, G.G., Einicker-Lamas, M., Allodi, S., 2007. Catalase, Bax and p53 expression in the visual system of the crab Ucides cordatus following exposure to ultraviolet radiation. Cell Tissue Res. 329, 159–168.
Mihaylova, M.M., Shaw, R.J., 2011. The AMPK signalling pathway coordinates cell growth, autophagy and metabolism. Nat. Cell Biol. 13, 1016–1023.
Miyakawa, H., Toyota, K., Hirakawa, I., Ogino, Y., Miyagawa, S., Oda, S., Tatarazako, N., Miura, T., Colbourne, J.K., Iguchi, T., 2013. A mutation in the receptor Methoprene-tolerant alters juvenile hormone response in insects and crustaceans. Nat. Commun. 4.
Motulsky, H.J., Brown, R.E., 2006. Detecting outliers when fitting data with nonlinear regression - a new method based on robust nonlinear regression and the false discovery rate. Bmc Bioinformatics 7.
Nandi, D., Tahiliani, P., Kumar, A., Chandu, D., 2006. The ubiquitin-proteasome system. J. Biosci. 31, 137–155.
Niki, E., 2008. Lipid peroxidation products as oxidative stress biomarkers. Biofactors 34, 171–180.
OECD, 2012. OECD Guideline for the Testing of Chemicals, *Daphnia magna* Reproduction Test. OECD.
Olzmann, J.A., Carvalho, P., 2019. Dynamics and functions of lipid droplets. Nat. Rev. Mol. Cell Biol. 20, 137–155.
Pacifici, R.E., Davies, K.J., 1991. Protein, lipid and DNA repair systems in oxidative stress: the free-radical theory of aging revisited. Gerontology 37, 166–180.
Parisot, F., Bourdineaud, J.P., Plaire, D., Adam-Guillermin, C., Alonzo, F., 2015. DNA alterations and effects on growth and reproduction in Daphnia magna during chronic exposure to gamma radiation over three successive generations. Aquat. Toxicol. 163, 27–36.
Perkins, A.T., Das, T.M., Panzera, L.C., Bickel, S.E., 2016. Oxidative stress in oocytes during midprophase induces premature loss of cohesion and chromosome segregation errors. Proc. Natl. Acad. Sci. U. S. A. 113, E6823–E6830.
Pfaffl, M.W., 2001. A new mathematical model for relative quantification in real-time RT-PCR. Nucleic Acids Res. 29, e45.
Raffa, S., Scrofani, C., Valente, S., Micaloni, A., Forte, M., Bianchi, F., Coluccia, R., Geurts, A.M., Sciarretta, S., Volpe, M., Torrisi, M.R., Rubattu, S., 2017. In vitro characterization of mitochondrial function and structure in rat and human cells with a deficiency of the NADH: ubiquinone oxidoreductase Ndufc2 subunit. Hum. Mol. Genet. 26, 4541–4555.
Redza-Dutordoir, M., Averill-Bates, D.A., 2016. Activation of apoptosis signalling pathways by reactive oxygen species. Biochim. Biophys. Acta 1863, 2977–2992.
Rottenberg, H., Scarpa, A., 1974. Calcium-uptake and membrane-potential in mitochondria. Biochemistry 13, 4811–4817.
Sarapultseva, E.I., Dubrova, Y.E., 2016. The long-term effects of acute exposure to ionising radiation on survival and fertility in Daphnia magna. Environ. Res. 150, 138–143.
Schubiger, M., Wade, A.A., Carney, G.E., Truman, J.W., Bender, M., 1998. Drosophila EcR-B ecdysone receptor isoforms are required for larval molting and for neuron remodeling during metamorphosis. Development 125, 2053–2062.
Shim, H.J., Lee, E.M., Nguyen, L.D., Shim, J., Song, Y.H., 2014. High-dose irradiation induces cell cycle arrest, apoptosis, and developmental defects during drosophila oogenesis. PLoS One 9.
Smaili, S.S., Hsu, Y.T., Youle, R.J., Russell, J.T., 2000. Mitochondria in Ca2+ signaling and apoptosis. J. Bioenerg. Biomembr. 32, 35–46.
Smith, W.A., Gilbert, L.I., 1986. Cellular-regulation of ecdysone synthesis by the prothoracic glands of Manduca-Sexta. Insect Biochemistry 16, 143–147.
Song, Y., Salbu, B., Teien, H.C., Heier, L.S., Rosseland, B.O., Tollefsen, K.E., 2014. Dose-dependent hepatic transcriptional responses in Atlantic salmon (Salmo salar) exposed to sublethal doses of gamma radiation. Aquat. Toxicol. 156, 52–64.
Song, Y., Rundberget, J.T., Evenseth, L.M., Xie, L., Gomes, T., Hogasen, T., Iguchi, T., Tollefsen, K.E., 2016. Whole-organism transcriptomic analysis provides mechanistic insight into the acute toxicity of emamectin benzoate in *Daphnia magna*. Environ Sci Technol 50, 11994–12003.
Song, Y., Villeneuve, D.L., Toyota, K., Iguchi, T., Tollefsen, K.E., 2017. Ecdysone receptor agonism leading to lethal molting disruption in arthropods: review and adverse outcome pathway development. Environmental Science & Technology 51, 4142–4157.
Steinhauser, G., Brandl, A., Johnson, T.E., 2014. Comparison of the Chernobyl and Fukushima nuclear accidents: a review of the environmental impacts. Sci. Total Environ. 470, 800–817.
Sudhof, T.C., 2012. Calcium control of neurotransmitter release. Cold Spring Harb. Perspect. Biol. 4.
Szumiel, I., 2015. Ionizing radiation-induced oxidative stress, epigenetic changes and genomic instability: the pivotal role of mitochondria. Int. J. Radiat. Biol. 91, 1–12.
Tollefsen, K.E., Scholz, S., Cronin, M.T., Edwards, S.W., de Knecht, J., Crofton, K., Garcia-Reyero, N., Hartung, T., Worth, A., Patlewicz, G., 2014. Applying adverse outcome pathways (AOPs) to support integrated approaches to testing and assessment (IATA). Regul. Toxicol. Pharmacol. 70, 629–640.
Trijau, M., Asselman, J., Armant, O., Adam-Guillermin, C., De Schamphelaere, K.A.C., Alonzo, F., 2018. Transgenerational DNA methylation changes in *Daphnia magna* exposed to chronic gamma irradiation. Environ Sci Technol 52, 4331–4339.
Valković, V., 2019. Chapter 9 - monitoring accidentally released radionuclides in the environment. In: Valković, V. (Ed.), Radioactivity in the Environment, Second edition Elsevier, pp. 505–634.
Vandesompele, J., De Preter, K., Pattyn, F., Poppe, B., Van Roy, N., De Paepe, A., Speleman, F., 2002. Accurate normalization of real-time quantitative RT-PCR data by geometric averaging of multiple internal control genes. Genome Biol. 3 RESEARCH0034.
Varga, T., Czimmerer, Z., Nagy, L., 2011. PPARs are a unique set of fatty acid regulated transcription factors controlling both lipid metabolism and inflammation. Biochimica Et Biophysica Acta-Molecular Basis of Disease 1812, 1007–1022.
Walton, K.D., Freddo, A.M., Wang, S., Gumucio, D.L., 2016. Generation of intestinal surface: an absorbing tale. Development (Cambridge, England) 143, 2261–2272.

Won, E.J., Lee, J.S., 2014. Gamma radiation induces growth retardation, impaired egg production, and oxidative stress in the marine copepod Paracyclopina nana. Aquat. Toxicol. 150, 17–26.
Xie, L., Solhaug, K.A., Song, Y., Brede, D.A., Lind, O.C., Salbu, B., Tollefsen, K.E., 2019. Modes of action and adverse effects of gamma radiation in an aquatic macrophyte Lemna minor. Sci. Total Environ. 680, 23–34.
Yoshida, T., Goto, S., Kawakatsu, M., Urata, Y., Li, T.S., 2012. Mitochondrial dysfunction, a probable cause of persistent oxidative stress after exposure to ionizing radiation. Free Radic. Res. 46, 147–153.
Zorov, D.B., Juhaszova, M., Sollott, S.J., 2006. Mitochondrial ROS-induced ROS release: an update and review. Biochim. Biophys. Acta 1757, 509–517.
Zou, Z., Saha, T.T., Roy, S., Shin, S.W., Backman, T.W.H., Girke, T., White, K.P., Raikhel, A.S., 2013. Juvenile hormone and its receptor, methoprene-tolerant, control the dynamics of mosquito gene expression. Proc. Natl. Acad. Sci. U. S. A. 110, E2173–E2181.